

MEMS-BASED PILLARED SURFACE FOR HIGH-SPEED DROPLET MANIPULATION: FAILURE OF CASSIE-BAXTER MODEL

Kenichi Morimoto, Kenichi Fukumoto and Yuji Suzuki

Department of Mechanical Engineering, The University of Tokyo, Japan

ABSTRACT

Recently, applicability of the Cassie-Baxter (C-B) model has been questioned. Here we evaluate the C-B model in prediction of the static/dynamic superhydrophobicity of micro-pillared surface. We have examined the effect of the pitch on the contact angle hysteresis (CAH) and the contact line friction, which is often ignored in modeling the wetting behavior. It is shown from the analysis of the droplet speed in a liquid dielectrophoresis device that the present pillared surface can realize high-speed droplet manipulation due to significant reduction of the contact line friction.

KEYWORDS: Superhydrophobicity, Pillared surface, Cassie-Baxter state, CAH

INTRODUCTION

Previously, we have proposed a new low-voltage droplet manipulation method called “liquid dielectrophoresis on electret (L-DEPOE)” for dielectric liquids [1], in which droplet manipulation is realized with electret as an embedded virtual voltage source. However, the contact angle (CA) of dielectric liquid on solid surfaces is generally small, so that pillared surface with low adhesion and low friction is necessary to improve the droplet speed in L-DEPOE [2]. In the Cassie-Baxter (C-B) model [3], CA and CAH are expressed with the solid fraction f_s and the roughness factor r_f . However, its applicability is now questioned especially for the superhydrophobic state [4-6].

In the present study, we systematically investigate the effects of the pitch p and f_s to model the high-speed droplet motion on pillared surface. Also, we analyse the droplet motion in a modeled L-DEPOE device in order to estimate the droplet speed achievable with the present surface and to identify the dominant resistance force.

FABRICATION OF PILLARED SURFACE

Figure 1 shows the schematic of the present pillared surface. The present pillar structure is a set of cylindrical posts, characterized by the pillar diameter, d , the pillar depth, t , and, the pitch between adjacent pillars, p . The solid fraction f_s is defined as $f_s = \pi d^2 / 4 p^2$. In the C-B model [3], the equilibrium CA on air-trapped surfaces is formulated as a function of only f_s and r_f in the following equation:

$$\cos \theta_{CB} = r_f f_s \cos \theta_{smooth} + f_s - 1, \quad (1)$$

where θ_{CB} and θ_{smooth} represent the CA on the C-B and smooth surface, respectively. Accordingly, the C-B state with large CA and thus small CAH is expected to be achieved with small f_s .

Wu and Suzuki [2] reported that the Cassie-Baxter state collapses to the Wenzel state with the applied voltage as low as 7.4 V when $p = 40 \mu\text{m}$ and $f_s = 0.012$. Since the stability of the Cassie-Baxter state will be improved for the smaller pitch [2], the effect of p on the hydrophobicity is presently explored while keeping $f_s \sim 0.01$. We prototyped Si micro-pillar arrays with $p = 2 \sim 30 \mu\text{m}$. MEMS processes for the present pillared surface are: i) Si pillars are

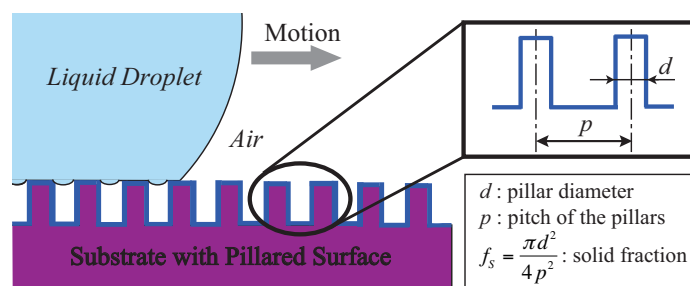


Figure 1. Superhydrophobic pillared surface for low friction and adhesion. Conventional models of contact angle and CAH depend only on the solid fraction f_s .

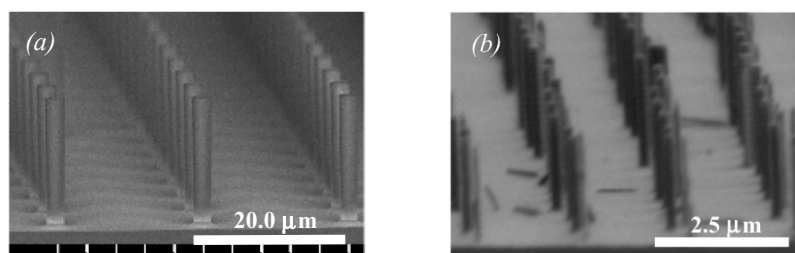


Figure 2. SEM images of MEMS-based pillared surfaces with $f_s = 0.01$: (a), $p = 20 \mu\text{m}$, (b) $p = 2 \mu\text{m}$.

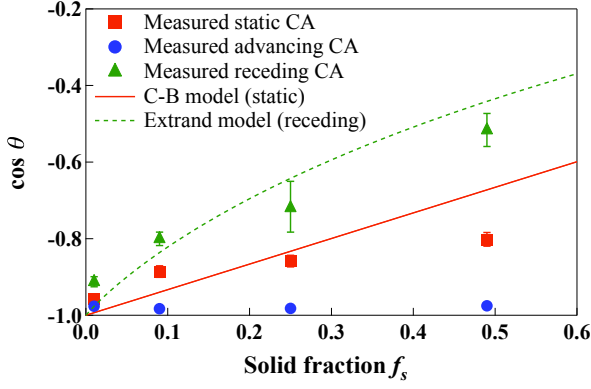


Figure 3. Static/advancing/receding contact angles versus f_s with $p = 2 \mu\text{m}$. Discrepancy with conventional models becomes obvious at small f_s .

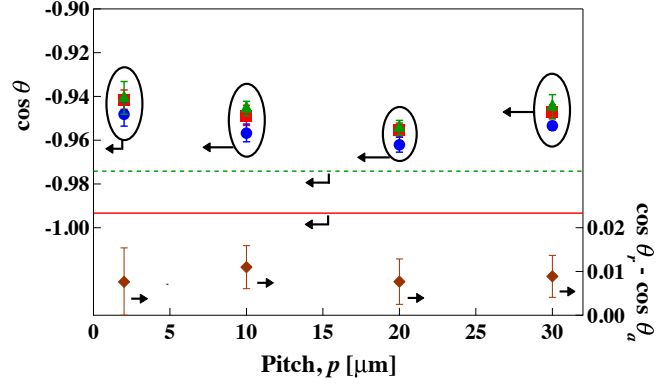


Figure 4. Contact angle and its hysteresis for different pitches with $f_s \sim 0.01$. The notation of each symbol and line for the left axis is the same as in Fig. 3.

microfabricated with EB lithography and DRIE, ii) 40 nm-thick hydrophobic C_xF_y film is deposited with C_4F_8 plasma onto the etched surface. Figure 2 shows SEM images of the pillars with different p .

RESULTS AND DISCUSSION

In the present study, DI water is employed as the droplet. From the measurement of the droplet on the surface with different solid fractions f_s , the contact angle becomes larger for smaller f_s . Figure 3 shows the static/receding/advancing CAs versus f_s . With decreasing f_s , the static CA increases and reaches 161° - 164° when $f_s = 0.01$. These trends of the CA data are different from the C-B model [3] prediction especially at low f_s . The discrepancy over the receding-CA model, proposed by Extrand [4], is also noticeably large. Figure 4 shows CA for different p with $f_s \sim 0.01$. With decreasing the pitch, both the static CA and the contact angle hysteresis (CAH), i.e., the difference between advancing and receding CAs, remain almost unchanged.

The coefficient of the contact line friction ζ [7] is also measured with sliding droplet experiments on inclined pillared surfaces, and estimated to be $\zeta = 8.07$, 0.026 , and 0.014 for the smooth surface, pillared surface with $p = 30 \mu\text{m}$ and $10 \mu\text{m}$, respectively. Thus, by decreasing the pitch while keeping f_s , the resistance would be significantly reduced. Since the existing wetting models [4, 6] are independent of p , the present results suggest that the pitch effect should be explicitly taken into account in the model.

Droplet motion in a modeled L-DEPOE device with the present pillared surface is examined. A water droplet is assumed to be sandwiched between top and bottom dielectric layers as shown in Fig. 5(a). As described in [1], the equation of motion of the droplet in the present capacitor model is expressed as:

$$m \frac{d^2x}{dt^2} = F_e + F_\mu + F_\theta = F_e + F_\mu + F_{th} + F_d, \quad (2)$$

where m is the mass of the droplet, and F_e , F_μ , and F_θ denote the driving force due to the potential gradient between the left and right electrodes, the viscous drag, and the CAH force, respectively. F_θ is divided into F_{th} and F_d , which represent the static and dynamic CAH force, respectively. For the pillared surface, each force exerted on a droplet (with its density ρ , surface tension γ , and the wetted area of width w and length l) is estimated as follows:

$$\begin{cases} F_e = -\partial(E_R + E_L)/\partial x, \\ F_\mu = 2lw f_s C_f \cdot \rho V^2 / 2, \\ F_{th} = 2w\gamma(\cos\theta_r - \cos\theta_a), \\ F_d = 4w\zeta V, \end{cases} \quad (3)$$

where E_R and E_L represent the electrostatic energy stored at the right and left parts of the capacitor, respectively. θ_a and θ_r represent the maximum and minimum static CAs. The skin friction coefficient C_f is given by $C_f = 1.328/\sqrt{Re}$ (Re is the Reynolds number based on the droplet velocity V and the distance between the top and bottom electrodes, h), assuming the Blasius solution of laminar boundary-layer flow.

Equation (2) is numerically integrated in time and the position and velocity of the droplet are obtained. The geometrical parameters are set to $w = l = b = 4.0 \text{ mm}$ (b is the length of the electrodes) and $h = 150 \mu\text{m}$, which correspond to a droplet volume of $2.4 \mu\text{l}$. The external capacitance is assumed as $C_0 = 2.0 \text{ pF}$. In Fig. 5(b), the terminal droplet velocity for each surface is shown for different applied voltage. It is seen that the droplet speed on the pillared surface is much increased and reaches 1 m/s with 300 V . In Fig. 5(c), each component of the resistance force is plotted against the droplet velocity for the pillared surface with $p = 10 \mu\text{m}$. Although static CAH (F_{th}) is the dominant resistance force for low droplet speed, the contact line friction (F_d) becomes dominant when the droplet speed is higher than 30 mm/s . Thus, further reduction of the contact line friction would be a key to high-speed droplet manipulation.

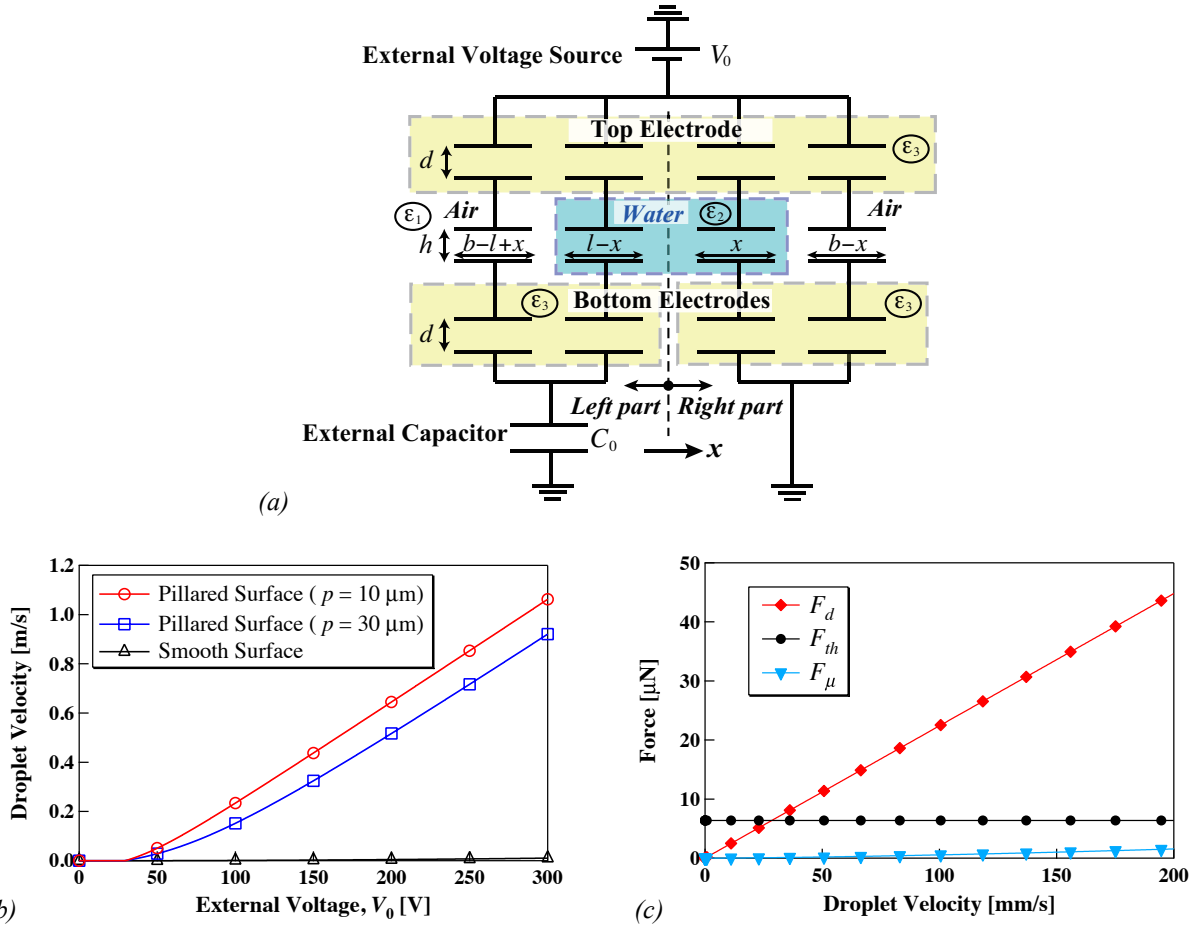


Figure 5. Evaluation of droplet speed in a modeled L-DEPOE device with the pillar surfaces ($f_s=0.01$): (a) Capacitor model (the dielectric constants of air, water, and electrodes are $\epsilon_1 = 1.0$, $\epsilon_2 = 80.0$, and $\epsilon_3 = 3.1$, respectively), (b) Droplet speed versus surface potential, (c) Resistance forces versus droplet speed for the pillared surface with $p = 10 \mu\text{m}$, in which the contact line friction is the major source of resistance.

CONCLUSION

We have evaluated the C-B model in prediction of the static/dynamic superhydrophobicity on micro-pillared surfaces. We examined the effect of the pitch on contact angle hysteresis and the contact line friction. It is concluded from the present results that the conventional C-B model without the pitch effect is not appropriate for its use to design pillared surfaces for high-speed droplet manipulation. From the analysis of the droplet motion in a modeled L-DEPOE device, it is shown that the present pillared surface with small pitch can realize extremely high speed up to 1 m/s due to the significant reduction of the contact line friction.

REFERENCES

- [1] T. Wu, Y. Suzuki, N. Kasagi, J. Micromech. Microeng., 20(8), 085043 (2010).
- [2] T. Wu, Y. Suzuki, Lab Chip, 11(18), pp. 3121-3129 (2011).
- [3] A. B. D. Cassie, S. Baxter, Trans. Faraday Soc., 40, pp. 546-551 (1944).
- [4] C. W. Extrand, Langmuir, 18(21), pp. 7991-7999 (2002).
- [5] L. Gao, T. J. McCarthy, Langmuir, 23(7), pp. 3762-3765 (2007).
- [6] M. Reyssat, D. Quéré, J. Phys. Chem. B, 113(12), pp. 3906-3909 (2009).
- [7] T. D. Blake, J. Colloid Interface Sci., 299(1), pp. 1-13 (2006).

CONTACT

Kenichi Morimoto, morimoto@mesl.t.u-tokyo.ac.jp